


Spontaneous generation of diversity in *Arachis* neopolyploids (*Arachis ipaënsis* × *Arachis duranensis*)^{4x} replays the early stages of peanut evolution

Soraya C. M. Leal-Bertioli ^{1,2,*} Eliza F. M. B. Nascimento,^{3,4} M. Carolina F. Chavarro,¹ Adriana R. Custódio,³ Mark S. Hopkins,¹ Márcio C. Moretzsohn,³ David J. Bertioli,^{1,5} and Ana Claudia G. Araújo³

¹Institute of Plant Breeding, Genetics and Genomics, Athens, GA 30602-6810, USA

²Department of Plant Pathology, University of Georgia, Athens, GA 30602, USA

³Embrapa Genetic Resources and Biotechnology, Brasília, 70770-917, Brazil

⁴Institute of Biological Sciences, University of Brasília, Brasília, 70910-000, Brazil, and

⁵Department of Crop and Soil Science, University of Georgia, Athens, GA 30602-6810, USA

*Corresponding author: Center for Applied Genetic Technologies, University of Georgia, 111 Riverbend Road, Athens, GA 30602-6810, USA. Email: sorayab@uga.edu

Abstract

Polyploidy is considered a driving force in plant evolution and domestication. Although in the genus *Arachis*, several diploid species were traditionally cultivated for their seeds, only the allotetraploid peanut *Arachis hypogaea* became the successful, widely spread legume crop. This suggests that polyploidy has given selective advantage for domestication of peanut. Here, we study induced allotetraploid (neopolyploid) lineages obtained from crosses between the peanut's progenitor species, *Arachis ipaënsis* and *Arachis duranensis*, at earlier and later generations. We observed plant morphology, seed dimensions, and genome structure using cytogenetics (FISH and GISH) and SNP genotyping. The neopolyploid lineages show more variable fertility and seed morphology than their progenitors and cultivated peanut. They also showed sexual and somatic genome instability, evidenced by changes of number of detectable 45S rDNA sites, and extensive homoeologous recombination indicated by mosaic patterns of chromosomes and changes in dosage of SNP alleles derived from the diploid species. Genome instability was not randomly distributed across the genome: the more syntenic chromosomes, the higher homoeologous recombination. Instability levels are higher than observed on peanut lines, therefore it is likely that more unstable lines tend to perish. We conclude that early stages of the origin and domestication of the allotetraploid peanut involved two genetic bottlenecks: the first, common to most allotetraploids, is composed of the rare hybridization and polyploidization events, followed by sexual reproductive isolation from its wild diploid relatives. Here, we suggest a second bottleneck: the survival of the only very few lineages that had stronger mechanisms for limiting genomic instability.

Keywords: *Arachis*; cytogenetics; domestication; genome instability; homoeologous recombination; neopolyploids; SNPs; polyploidy; morphology

Introduction

Polyploidy is near universal in plants: over evolutionary time, all, or almost all angiosperms have undergone at least one polyploidization event, also known as a whole-genome duplication (Wendel 2015). In addition, about half of all higher plant species have undergone more recent polyploidization (Soltis et al. 2015). Polyploidy has long been viewed as advantageous: it provides heterosis and gene redundancy and brings enhanced novelty that can broaden phenotypic plasticity providing the ability to adapt to new ecological niches (Comai 2005; Soltis et al. 2015; Blaine Marchant et al. 2016; Soltis and Soltis 2016; Van de Peer et al. 2017). Crosses between individuals with different ploidy levels usually result in sterile offspring, therefore, polyploidy precipitates speciation between the new polyploid and its associated progenitor diploids (Ramsey and Schemske 1998; Adams and Wendel 2005). Two main types of polyploidy can be identified:

autopolyploidy, the duplication of the chromosome set of one species, and allopolyploidy, the merger of genomes from different species into a single nucleus, and whole-genome duplication (Stebbins 1971; Wendel and Doyle 2005; Mason and Wendel 2020). The initial stage of allopolyploidization, involving sudden changes due to the merge of different genomes, has been classically known as “genetic shock” (McClintock 1984). This includes genetic, epigenetic, and gene expression changes. These changes can occur rapidly, as early as in somatic cells of interspecific F₁ hybrids, or in the generations following chromosome doubling. Examples of successful allopolyploid modern species are rapeseed, coffee, tobacco, cotton, and peanut (Kochert et al. 1996; Leitch et al. 2008; Yoo et al. 2013; Chalhoub et al. 2014; Lashermes et al. 2014).

The allotetraploid peanut (*Arachis hypogaea* L.) belongs to the genus *Arachis* that has 83 described species, divided into nine

Received: June 04, 2021. Accepted: August 01, 2021

© The Author(s) 2021. Published by Oxford University Press on behalf of Genetics Society of America.

This is an Open Access article distributed under the terms of the Creative Commons Attribution License (<http://creativecommons.org/licenses/by/4.0/>), which permits unrestricted reuse, distribution, and reproduction in any medium, provided the original work is properly cited.

taxonomical sections (Valls and Simpson 2005, 2017; Krapovickas and Gregory 2007; Valls et al. 2013; Santana and Valls 2015; Seijo et al. 2021). Peanut belongs to the section *Arachis*. The section has six recognized genome types, based on the distribution patterns of heterochromatic bands and rDNA loci: A, B, D, F, G, and K-genome types, with two basic chromosome numbers ($x=10$ and $x=9$), and two ploidy levels ($2x$ and $4x$) (Smartt and Gregory 1967; Stalker 1991; Seijo et al. 2004; Robledo and Seijo 2008, 2010; Robledo et al. 2009; Silvestri et al. 2015). Peanut is an allotetraploid with an AABB type genome, $2n=4x=40$ (Husted 1936), that arose from one or a very few events of hybridization and tetraploidization (Kochert et al. 1996; Bertioli et al. 2019). Cytogenetic, phylogeographic and molecular evidence indicate *Arachis duranensis* Krapov. & W.C. Greg. and *Arachis ipaënsis* Krapov. & W.C. Greg. as the A and B subgenomes parents of peanut, respectively (Kochert et al. 1996; Seijo et al. 2004, 2007; Ramos et al. 2006; Robledo et al. 2009; Lavia et al. 2011; Grabilele et al. 2012; Moretzsohn et al. 2013). These two species diverged 2–3 Mya (Moretzsohn et al. 2013; Bertioli et al. 2016). Hybridization of *A. duranensis* and *A. ipaënsis*, spontaneous polyploidy (about 5000 and 10,000 years ago), and domestication gave rise to the modern crop (Bertioli et al. 2016, 2019, 2020). The initial genome duplication event isolated the new allopolyploid from all other diploid *Arachis* species. DNA evidence indicates a very narrow polyploid origin that generated a significant bottleneck (Bertioli et al. 2019; Yin et al. 2020). Despite this, peanut has evolved into diverse growth habits, architecture, and morphological forms; shorter and longer growing seasons; different testa colors and numbers of seeds per pod, and different hues and patterning of flowers. Two subspecies of *A. hypogaea* are recognized, *hypogaea* and *fastigiata* between which, remarkably, there is partial sexual incompatibility. The two subspecies have two (*hypogaea* and *hirsuta*) and four (*fastigiata*, *vulgaris*, *aequatoriana*, and *peruviana*) botanical varieties, respectively (Krapovickas and Gregory 2007). Even though several diploid *Arachis* species were cultivated before the tetraploid, only the latter fully developed a domestication syndrome and was dispersed around the globe to become a crop of worldwide importance (See Supplementary Note 1 in Bertioli et al. 2019). This strongly implicates polyploidy as a significant factor for niche expansion into domestication and subsequent success as a crop plant, perhaps driven by increased evolutionary phenotypic plasticity, and ability to adapt to different environments. Here, we investigated induced allotetraploids generated from peanut's progenitor species with the rationale that they likely replay the initial genetic events following the origin of *A. hypogaea* and its wild counterpart of common origin, the allotetraploid *Arachis monticola*.

Both progenitor species are extant and were recently sequenced (Bertioli et al. 2016). The B genome donor, *A. ipaënsis*, is nowadays represented by only a single accession, K 30076. Biogeography indicates that it was moved by humans in prehistory into the range of the A subgenome donor, thus enabling the formation of the allotetraploid species. Extraordinary DNA identity (modal values of 99.98%) between *A. ipaënsis* and the B subgenome of peanut indicate that it likely descended from the very same population that gave rise to peanut in a very recent polyploidy event (Bertioli et al. 2016; Yin et al. 2020). The sequenced representative of the A subgenome donor species, *A. duranensis* V 14167, is also very close to the A subgenome of cultivated peanut, with modal identity around 99.75% (Bertioli et al. 2020). The availability of such close representatives of the ancestors of cultivated peanut provides us with remarkable opportunities to “replay” the origin of *A. hypogaea*. Here, we used lineages from two independent induced polyploidy events (Favero et al. 2006; Bertioli et al.

2019), spanning 11 generations. These induced allopolyploids spontaneously generated phenotypic and genome diversity, in a way that likely mimics events that occurred between about 5000 and 10,000 years with the spontaneous origin of tetraploid peanut: the first bottleneck, the polyploidization, that isolated the original allotetraploid from the wild diploid relatives, and the second bottleneck proposed here, is the control of genomic instability allowing survival of few lineages.

Materials and methods

Plant material

Lineages from two independent induced allotetraploids (neopolyploids) were used in this study, both derived from crosses between accessions of the peanut's progenitor species *A. ipaënsis* K 30076 (female), and *A. duranensis* V 14167 (male). These were also the accessions used to construct the diploid reference genomes (Bertioli et al. 2016). Although all evidence points to *A. duranensis* being the female progenitor (Kochert et al. 1996; Grabilele et al. 2012), its delicate flower and other unknown factors have prevented any AB hybrid from being produced, with a unique exception, very recently published (García et al. 2020). Diploid BA hybrids were treated with colchicine for chromosome doubling, as described in Leal-Bertioli et al. (2017). Lineages from the neopolyploid obtained by Favero et al. (2006) are here termed IpaDur1. IpaDur1 was propagated and maintained for nine generations of self-pollination, without intentional selection, regardless of morphological aspects, pollen viability, or fertility. The neopolyploid obtained years later using the same parents (Bertioli et al. 2019) is here termed IpaDur2. Different independent lineages of two generations (S_2 and S_3) from a single hybrid IpaDur2 were studied individually. These and all other genotypes used in this study are listed on Table 1.

Plant phenotyping

In order to investigate phenotypic variation between different allotetraploids produced from the same diploid hybrid, general traits were observed (plant habit, main stem height, and leaf size) and seed width and length were measured from 16 IpaDur2 plants at S_2 (second generation of self-pollination). For comparison, *A. duranensis* and *A. ipaënsis* seeds were also measured. Data were analyzed using the Shapiro–Wilk test for normality. For comparing groups, ANOVA (parametric) or Kruskal–Wallis test (nonparametric) were used. Variance of each group was compared using the Levene's test for equality of variances (Levene 1960). All tests and plots were performed using R package. The color of the flowers of the 16 IpaDur2 S_2 plants was determined at onset of anthesis.

Cytogenetic analysis

Chromosome preparations:

Cytogenetic analyses were performed on samples of both induced allotetraploids, IpaDur1 S_{10} (10th generation of self-pollination), IpaDur2 S_2 (2nd generation of self-pollination). Root tips were isolated from at least five plants of each IpaDur2 and IpaDur1. At least 10 metaphases of each plant (over 250 metaphases per genotype) were observed. Root tips (5–10 mm long) from 4-week-old plants were collected, treated with 2 mM 8-hydroxyquinoline for 2 h at room temperature and another hour at 4°C with new solution, and then incubated in fixative solution (absolute ethanol: glacial acetic acid, 3:1, v/v) for 12 h at 4°C. Somatic chromosome spreads were prepared according to Schwarzacher and Heslop-Harrison (2000) with few modifications: meristems were digested

Table 1 Wild, cultivated, and induced allotetraploid *Arachis* genotypes used for phenotypic, cytogenetic, and genotypic analyses

Genotype	Plant ID	Ploidy	Genome type	Collection site
Wild species				
<i>A. duranensis</i> Krapov. & W.C. Greg.	V 14167	2x	AA	Salta, Argentina
<i>A. ipaënsis</i> Krapov. & W.C. Greg.	K 30076	2x	BB	Gran Chaco, Bolivia
<i>A. monticola</i> Krapov. & Rigoni	V 14165	4x	AABB	Jujuy, Argentina
Cultivated peanut				
<i>A. hypogaea</i> L. subsp. <i>fastigiata</i> Waldron var. <i>fastigiata</i>	"IAC-Tatu-ST"	4x	AABB	Modern cultivar
Induced allotetraploids				
[<i>A. ipaënsis</i> K30076 × <i>A. duranensis</i> V14167] ^{4x}	IpaDur1a	4x	BBAA	Induced allotetraploid at generations S ₁ to S ₁₀
[<i>A. ipaënsis</i> K30076 × <i>A. duranensis</i> V14167] ^{4x}	IpaDur2b	4x	BBAA	Induced allotetraploid at generations S ₂ and S ₃

^a Favero et al. (2006).^b Bertioli et al. (2019).

in 10 mM citrate buffer containing 2% cellulase (from *Trichoderma viridae*; Onozuka R-10 Serva) and 20% pectinase (from *Aspergillus niger*, Sigma) for 2 h at 37°C. Chromosomes of each root were set on a slide, in a drop of acetic acid 45% and the spread was obtained by applying pressure to coverslip. Slides were selected using phase contrast in the Axioskop microscope (Zeiss, Oberkochen, Germany). Coverslips were removed, slides were air-dried for 24 h and kept at -20°C.

CMA3+/DAPI heterochromatic banding

CMA₃⁺/DAPI banding was conducted with IpaDur1 S₁₀ and IpaDur2 S₂ plants following (Schweizer and Ambros 1994) to localize GC and AT-rich heterochromatic regions, respectively. Chromosome spreads were treated with 0.5 mg/ml of chromomycin A3 (CMA₃) for 1 h at room temperature, then with 2 µg/ml of 4', 6-diamino-2-phenylindole (DAPI) for 30 min at room temperature. Slides were mounted with glycerol/McIlvaine buffer and analysis was conducted in the epifluorescence Zeiss AxioPhot photomicroscope (Zeiss, Oberkochen, Germany). Images were captured using Zeiss AxioCam MRc digital camera (Zeiss Light Microscopy, Göttingen, Germany) and AxioVision Rel. 4.8 software and further processed using the Adobe Photoshop CS10 software, applying only functions that affect the whole image equally. At least 50 metaphases of each plant (250 metaphases per genotype) were observed.

In situ hybridization—FISH and GISH

Production of probes

Probes for genomic *in situ* hybridization (GISH) were obtained from genomic DNA (1 µg) isolated from young leaflets of *A. duranensis* and *A. ipaënsis*, using a CTAB protocol (Doyle and Doyle 1987). Purified DNA (1 µg) was labeled with either, digoxigenin-11-dUTP (Roche Diagnostics Deutschland GmbH) or Cy3-dUTP (Roche Diagnostics Deutschland GmbH) by Nick Translation kit (Roche Diagnostics Deutschland GmbH). For fluorescent *in situ* hybridization (FISH), we used clones containing the sequences corresponding to 5S ribosomal DNA of *Lotus japonicus* (Pedrosa et al. 2002) and 18S-5.8S-25S of *Arabidopsis thaliana* (Wanzenböck et al. 1997). The rDNA was isolated with the Illustra plasmid Prep Midi Flow kit (GE Heltcare) and rDNA sequences were labeled by Nick translation, using the same kits as described for the genomic probes.

Hybridization

The *in situ* hybridization experiments were performed as described by Schwarzacher and Heslop-Harrison (2000). Hybridization steps and conditions were identical for GISH and FISH experiments. The slides with metaphase spreads were pre-

treated with 10 mg/ml RNase A for 1 h at 37°C, followed by treatment with pepsin (10 mg/ml) for 15 min at 37°C. Slides were incubated in fixative solution containing 4% paraformaldehyde for 10 min at room temperature.

Double GISH used both genomic probes together (*A. duranensis* and *A. ipaënsis*-derived probes, ~50 ng of each probe/slide). Hybridizations were performed for 14 h at 37°C, followed by 73% stringent washes, using 2x saline citrate buffer (SSC). Hybridization sites were immunocytochemically detected using the antibody anti-digoxigenin conjugated to fluorescein (Roche Diagnostics Deutschland GmbH) or by direct observation of the Cy3 fluorescence in the epifluorescence microscope Zeiss AxioPhot (Zeiss, Oberkochen, Germany). Slides were counterstained with DAPI before observation.

SNP genotyping and data analysis

For allotetraploid plants, genetic exchange occurs mainly between chromosomes that are part of the same subgenome, i.e., homologous exchanges. However, it was previously noted that a proportion of these genetic exchanges happen between different subgenomes (homeologous exchanges). In the case of peanut allotetraploids, the products of homeologous recombination form the genome configurations AAAA and BBBB (Leal-Bertioli et al. 2015, 2019). Here, we characterized this phenomenon using (1) different generations and (2) different lineages of allotetraploid plants. Different generations consisted of seeds of selfed IpaDur1 collected from 2007 to 2016 (S₁ to S₁₀). Different lineages of allotetraploid plants from the same hybridization event comprised 15 S₂ plants and one S₃ plant of the tetraploid IpaDur2. All these plants from different generations of IpaDur1 and different lineages of IpaDur2 were genotyped and compared. Single plants were genotyped from each lineage/each generation.

Genomic DNA was extracted from young leaves using Qiagen Plant DNeasy kit (Qiagen, Germantown, MD, USA) and quantified by Qubit 4 fluorometer (ThermoFisher Scientific, Waltham, MA, USA). Genotyping was performed with the Axiom *Arachis* SNP array v02, a 48K SNP array, designed using machine-learning models as described by Korani et al. (2019). The reference genomes used for the array design were of *A. duranensis* accession V 14167 and *A. ipaënsis* K 30076 (Bertioli et al. 2016), the same accessions and the same genetic stocks as used to make the neopolyploids used in this study. Total sizes of genome assemblies were 1211 and 1512 Mb for *A. duranensis* and *A. ipaënsis*, respectively. Total repetitive contents were estimated as 61.7 and 68.5% for the *A. duranensis* and *A. ipaënsis*, respectively (Bertioli et al. 2016). Progenitors were genotyped as controls. Genotyping results were analyzed with the Axiom Analysis Suit (ThermoFisher Scientific). Each sample was

replicated at least once. Data were filtered by quality using the QC call rate >90%. The genotyping information was filtered allowing a minor allele frequency (MAF) >0.05 and 20% missing calls. Markers showing inconsistent calls from duplicates of the same sample were discarded. Data output was visualized in Microsoft Excel. Genotyping with the Axiom Array gives results which are consistent with genotyping by sequencing. For instance, we have directly compared results from the genotyping by sequencing illustrated in Bertoli et al. (2019) (Figure 1, left hand panels, A and B). Axiom genotyping was much more cost effective, and therefore, we used it in this study.

Results

Morphology

IpaDur1, produced before 2006, was propagated and maintained for nine generations of self-pollination, without intentional selection, regardless of morphological aspects, pollen viability, seed set or evidence of alterations in genome stability i.e., all viable seeds were collected. All tetraploid plants had larger leaves and flowers than those of the diploid parents, but similar trailing habit and average seed size to the diploid parents (Figure 1, A-F, Leal-Bertioli et al. 2017). Most lineages had yellow flowers, but a few had orange flowers.

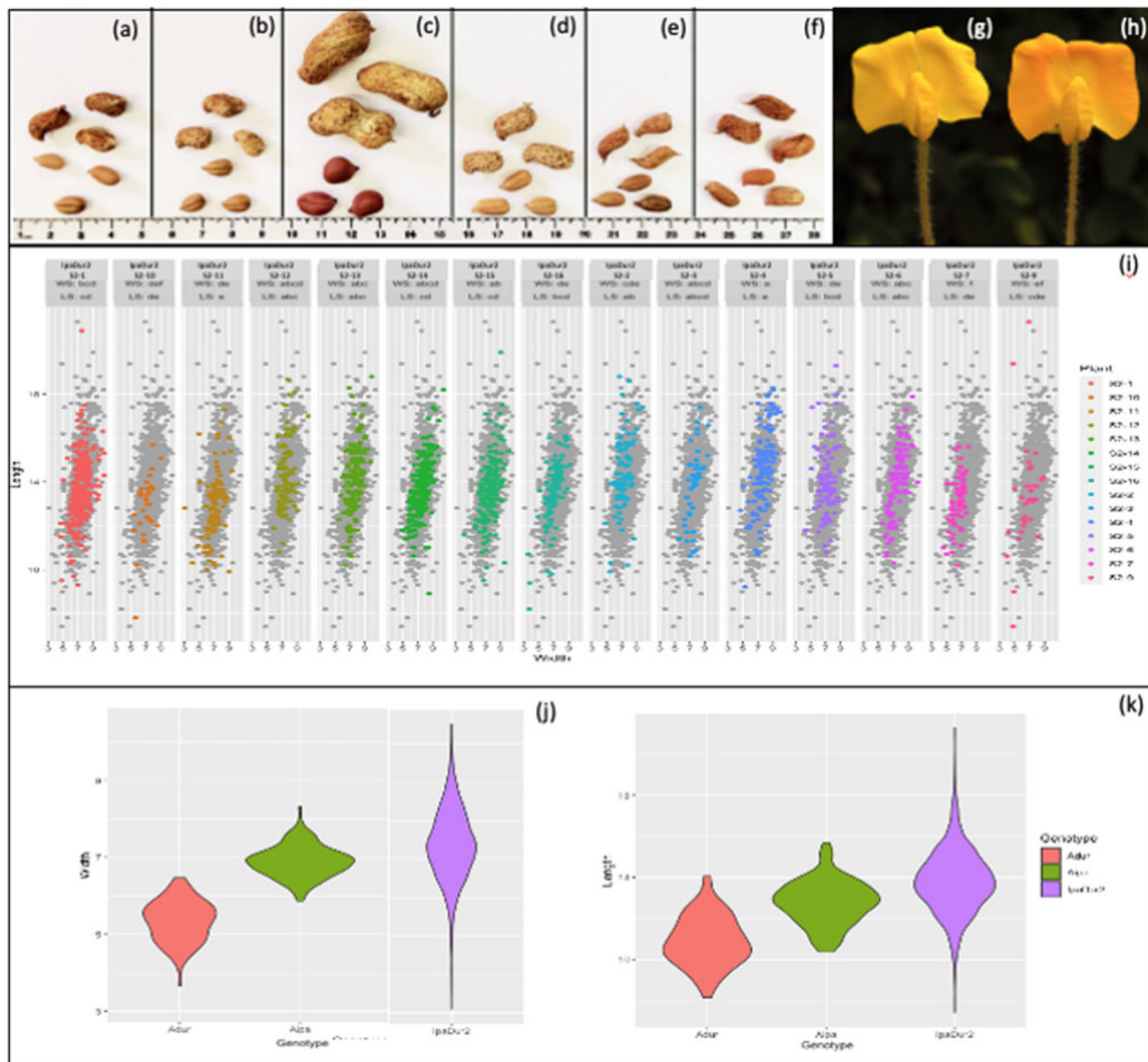


Figure 1 (A-F) Pods and seeds of *Arachis* genotypes used in this study. IpaDur2 (*A. ipaënsis* K 30076 × *A. duranensis* V 14167)^{4x} (A); IpaDur1 (*A. ipaënsis* K 30076 × *A. duranensis* V 14167)^{4x} (B); *A. hypogaea* subsp. *fastigiata* var. *fastigiata* “IAC Tatu-ST” (C); *A. monticola* (V 14165) (d); *A. duranensis* (V 14167) (E) and *A. ipaënsis* (K 30076) (F). Scale: cm. (G, H): Yellow (G) and orange (H) flowers from the induced allotetraploid IpaDur2 (*A. ipaënsis* K 30076 × *A. duranensis* V 14167)^{4x}. Bar: 5 mm. (I-K) Distribution of seed length (y-axis) and width (x-axis) values, in mm, across 15 IpaDur2 S₂ plants. Distribution of entire phenotypic data of IpaDur2 plants in the background of the scatterplots and distribution of each plant is indicated by colors. Letters on top indicate significant difference among plants for seed length (LS) and width (WS) (P-value ≥ 0.05) (i) Violin plots show the distribution and data density for seed width and length from *A. duranensis*, *A. ipaënsis* and IpaDur2 (j, k).

The first-generation seeds of the neopolyploid IpaDur2 (S_1) had low-germination rate: from the over 50 seeds produced, only 16 germinated. This contrasts with the diploid parents, that have typically over 90% germination rate. The IpaDur2 plants had very similar traits to IpaDur1 (Figure 1). All S_2 IpaDur2 plants produced yellow flowers, but in the subsequent generation, S_3 , one individual produced orange flowers (Figure 1, G and H). The number of pods produced varied widely among the individuals, ranging between one and 103 pods per plant. Seed size differed significantly among individuals according to the nonparametric Kruskal-Wallis test (Figure 1I). Levine test of variance revealed a P -value greater than 0.05, indicating that there was significant difference in variance between the genotypes: Variance of seed width and length of IpaDur2 was higher than *A. duranensis* and *A. ipaënsis* (Figure 1, J and K, Supplementary File S1). Overall, the IpaDur2 lineages we studied here had slightly more variability in seed size than IpaDur1. Both IpaDur1 and IpaDur2 plants presented a general variability in number and length of branches, main stem height, leaf color among other features, but it is difficult to assign statistical significance to this variability because each plant is an individual.

Cytogenetic characteristics

Chromosome morphology

The correspondence between chromosomal pseudomolecule numbering (Bertioli et al. 2016) and cytogenetic numbering (Seijo et al. 2004, 2007; Lavia et al. 2008; Robledo and Seijo 2008, 2010; Robledo et al. 2009; Grabile et al. 2012) is so far mostly unknown in *Arachis* (Bertioli et al. 2019). Therefore, herein, to avoid confusion, we will specify the cytogenetic nomenclature with the prefix “cyt-*X,” with an asterisk (*) referring to the type of the subgenome (A or B) and X, the corresponding number of the chromosome. The neotetraploids IpaDur2 and IpaDur1 harbored 40 chromosomes, comprising 36 metacentric and four submetacentric, which corresponds to the sum of those of the diploid parental species, *A. ipaënsis* and *A. duranensis*. In all sets of chromosomes analyzed, a small pair “A” and one satellite chromosome were identified (Figure 2, A and B). The small pair “A” corresponds to the pair of chromosomes cyt-A9* in *A. duranensis*, characterized by a remarkably high condensation level of the heterochromatin on the centromeres. In addition, the pair of

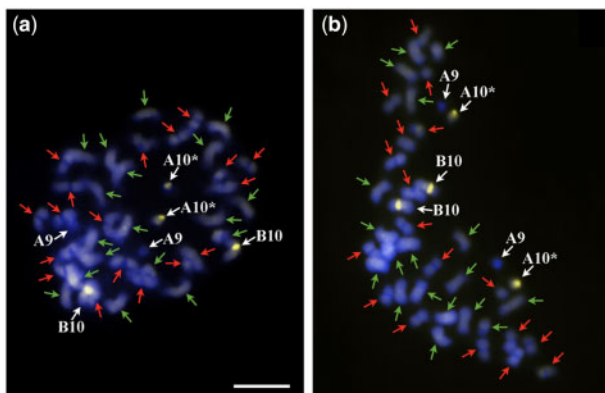


Figure 2 General overview of chromosomes of IpaDur2 S_2 (A) and IpaDur1 S_{10} (B). Both genotypes showing CMA_3^+ bands (yellow) on proximal regions of cyt-A10 (A10) and cyt-B10 (B10). Chromosomes of A subgenome are indicated by green arrows (faded DAPI bands on centromeres) and chromosomes of B subgenome, by red arrows. Cyt-A10 shows secondary constriction and a short arm and a proximal segment of the long arm (*). Bar: 5 μ m.

chromosomes with a secondary constriction and satellite segment near to the proximal segment of the long arm of the chromosome corresponds to the pair of chromosomes cyt-A10 in *A. duranensis* (Figure 2).

Distribution of heterochromatic bands

IpaDur2 and IpaDur1 had conspicuous DAPI+ bands on centromeric regions of the ten pairs of chromosomes of the A subgenome while the other 10 pairs from the B subgenome lacked these bands. These DAPI+ banding patterns in the induced tetraploids were indistinguishable from *A. hypogaea* and *Arachis monticola* and the same as expected for the sum of the diploid progenitors. This indicates the conservative organization of these chromosomal structures after allopolyploidization, in lineages formed at different times, induced and spontaneous (Figure 2).

CG-rich repetitive heterochromatic regions in the DNA that displayed CMA_3^+ bands were observed on the proximal regions of chromosomes cyt-A10 and cyt-B10 of both IpaDur2 S_2 and IpaDur1 S_{10} (Figure 2, A and B, respectively), corresponding to the sum of the bands of the parental species *A. duranensis* and *A. ipaënsis* (Nascimento et al. 2018). However, this pattern differed from the other two allotetraploids, *A. hypogaea* [with CMA_3^+ bands on cyt-A2, cyt-A10, cyt-B3, cyt-B7, and cyt-B10, (Nascimento et al. 2018)] and *A. monticola* [with CMA_3^+ bands only on cyt-A2 and cyt-A10 (Nascimento et al. 2020)]. These differences in CMA_3^+ band number and distribution may be due to changes in DNA sequence, or in the organization of the DNA that reduced binding of the fluorophore.

Affinity to progenitor genomes by GISH

GISH signals were present on all chromosomes of IpaDur1 and IpaDur2, for the corresponding subgenomes A and B. Double GISH, using both genomic probes on IpaDur2 (Figure 3, A–C) and IpaDur1 chromosomes (Figure 3, D–F) confirmed the preferential hybridization of the chromosomes of the *A. duranensis* probe to the A subgenome chromosomes (red, Figure 3, A and D) and of the *A. ipaënsis* probe to the B subgenome chromosomes (green, Figure 3, B and E) similarly to what has been shown for *A. hypogaea* and *A. monticola* (Seijo et al. 2007; Nascimento et al. 2018). Hybridization signals were weaker at chromosome terminal regions. However, for most chromosomes overlapping hybridization signals were observed, i.e., both probes hybridized to the same DNA region (yellow, Figure 3, C and F), indicating DNA sequences that are shared by subgenomes A and B. On both genotypes, there were mosaic hybridization patterns on cyt-B10 (green signal interspersed with red signals), indicating recombination between A and B subgenomes (Figure 3, C and F). Cyt-B10 also showed extensive yellow signals, indicating “invasion” of A alleles onto B genome chromosome.

Distribution of rDNA loci

The number, size, and position of the 5S rDNA loci on chromosomes of IpaDur2 and IpaDur1 were identical (Figure 6 and Nascimento et al. 2018). The loci were situated on the proximal region of chromosomes cyt-A3 and cyt-B3, along the short arms, as were observed in each diploid species, *A. duranensis* and *A. ipaënsis*, respectively, thus representing an additive character in both neopolyploids.

The 45S rDNA loci in IpaDur1 S_{10} (Figure 4A) consisted of two loci from *A. duranensis* (on cyt-A2 and cyt-A10) and just one locus out of three loci originally present in *A. ipaënsis* (on cyt-B10) thus not being an additive character (this was also observed in Nascimento et al. 2018). In IpaDur2 S_2 , two patterns of 45S rDNA

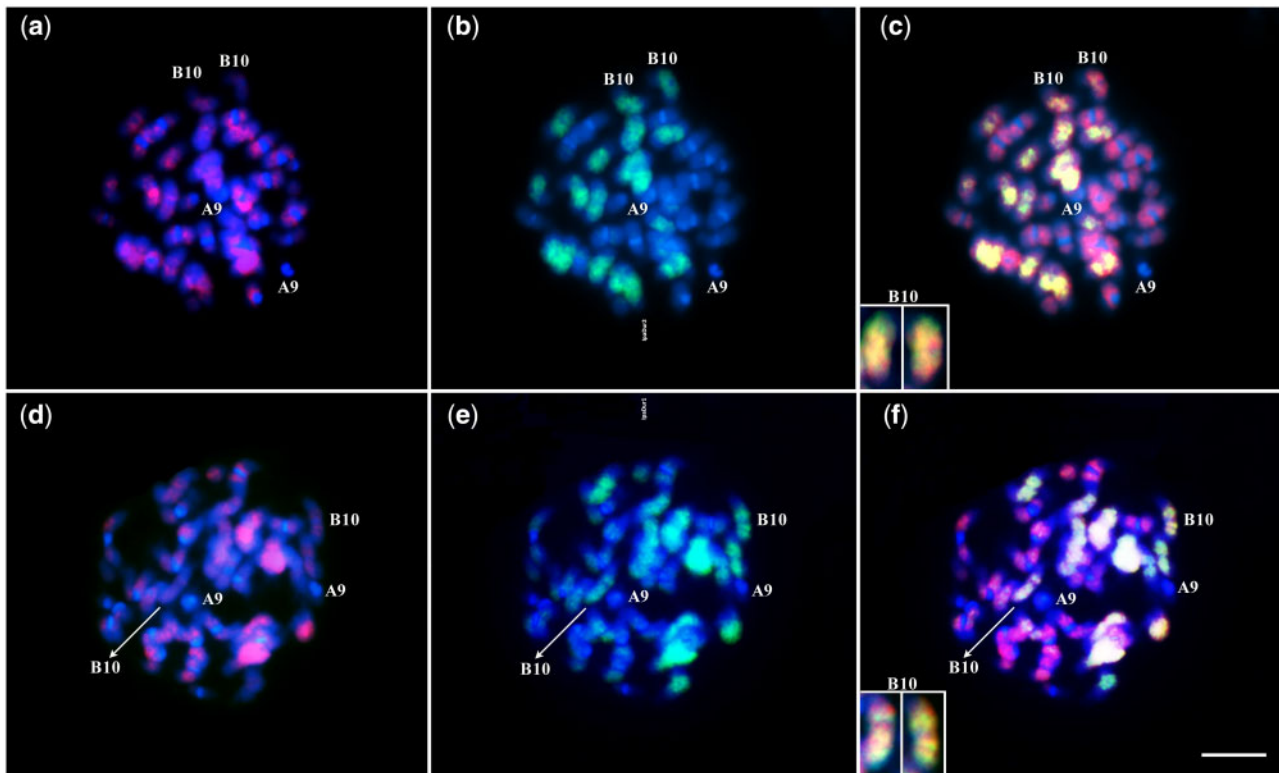


Figure 3 Double GISH in IpaDur2 S_2 (A–C) and IpaDur1 S_{10} (D–F) using simultaneously, *A. duranensis* (red) and *A. ipaënsis* (green) probes, followed by DAPI counterstaining (blue). Note the preferential affinity of *A. duranensis* probe (red) to chromosomes of the A subgenome showing DAPI+ bands on centromeres (A, D), and of *A. ipaënsis* probe (green) to chromosomes of the B subgenome, lacking DAPI bands (B, E). *A. duranensis* probe (red) also show some hybridization to chromosomes of the B subgenome, indicating genome inversion A to B. Many chromosomes have yellow signals, that result from the overlapping green and red sites indicating DNA sequences that are shared between A and B subgenomes, observed. Image insets of cyt-B10 show mosaic pattern of hybridization, indicating recombination between A and B subgenomes in IpaDur2 (C) and IpaDur1 (F). Bar = 5 μ m.

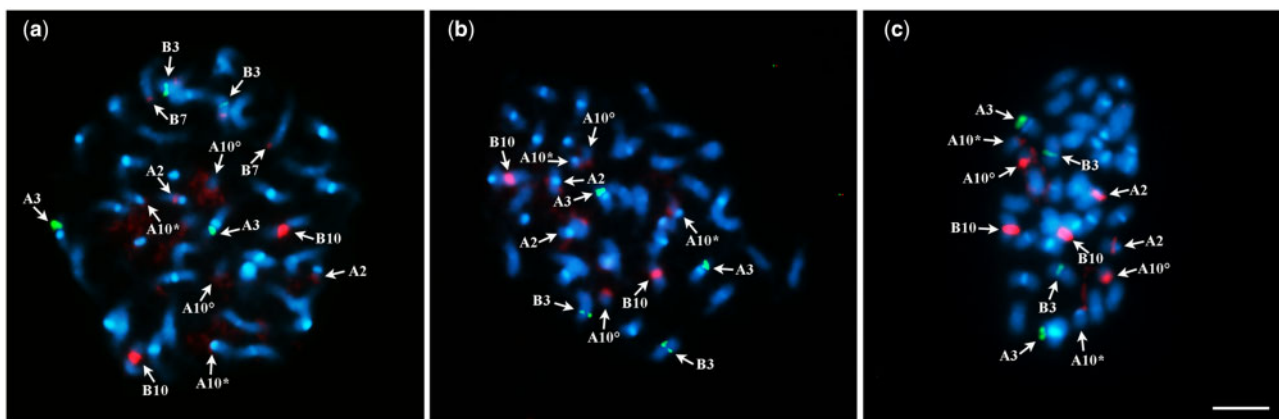


Figure 4 Double FISH on somatic metaphases of IpaDur1 S_{10} (A) and IpaDur2 S_2 (B, C) after double FISH using simultaneously, 5S ribosomal DNA (rdNA) (green) and 45S rDNA (red) probes, followed by DAPI counterstaining. Twenty chromosomes of the A subgenome have DAPI+ bands on centromeres (light blue). The 5S rDNA loci (green) are detected on cyt-A3 (A3) and cyt-B3 (B3) on both genotypes on all preparations (A–C). 45S rDNA (red) are detected on IpaDur1 on cyt-A2 (A2), cyt-A10 (A10), cyt-B10 (B10) (A). On IpaDur2, most metaphases show the same pattern (B), whereas some metaphases show two extra sites, on cyt-B3 (B3) and cyt-B7 (B7) (C). Cyt-A10 short arm and proximal segment of the long arm (*) and satellite (°). Bar: 5 μ m.

hybridization were observed: three of these loci were detected in all metaphases (proximal regions of cyt-A2 and cyt-B10 and near the secondary constriction of cyt-A10); the remaining two loci (proximal regions of cyt-B3 and cyt-B7 terminal regions, Figure 4C), on some individuals, presented weak or no detectable hybridization signals on others (Figure 4B). Notably, this

variability was observed not only between individuals, but also between cells of the same individual. Cyt-B3 showed colocalization of 5S and 45S loci, whilst cyt-A10 showed the largest rDNA 45S site (green), with an intense signal on the secondary constriction, and a thread-like aspect, characteristic of a NOR (Nucleoli Organizing Region). *A. hypogaea* and *A. monticola* have

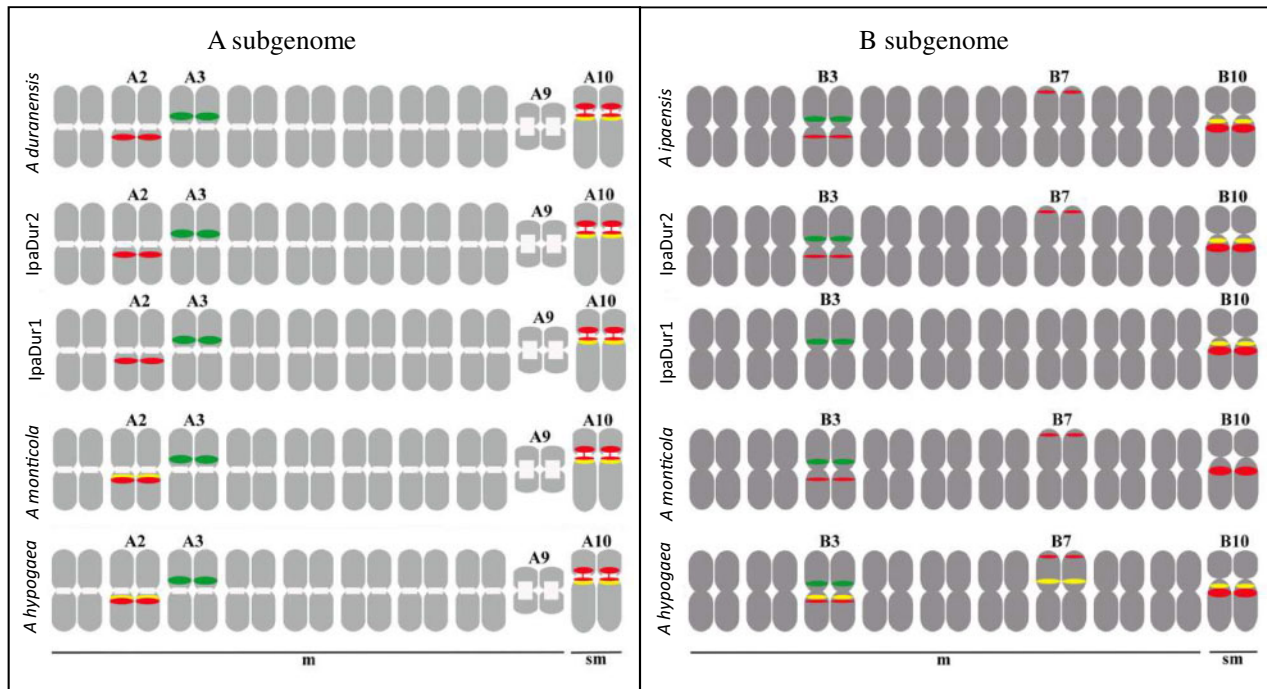


Figure 5 Schematic diagram of some *Arachis* karyotypes showing variability in chromosome morphology; centromeres (m, metacentric; sm, submetacentric); DAPI⁺ banding (white), CMA₃ bands (yellow), and 5S (green), and 45S (red) rDNA loci in *A. duranensis* V 14167, *A. ipaënsis* K 30076, IpaDur2, IpaDur1, *A. monticola* V 14165, and *A. hypogaea* “IAC-Tatu-ST” (from Nascimento et al. 2020). Variability is detected on cyt-A2, cyt-B3, cyt-B7, and cyt-B10. Only the most common configuration of IpaDur2 is presented.

five loci easily detected on the proximal region of the long arm of cyt-A2, cyt-A10, and proximal region of short arm of cyt-B3 and terminal region of the short arm of cyt-B7, corresponding to the sum of the two loci from *A. duranensis* and three from *A. ipaënsis* (Nascimento et al. 2020). All these results are summarized in Figure 5. The karyotypes of *A. hypogaea* subsp. *fastigiata* var. *fastigiata* “IAC Tatu-ST,” *A. monticola* (V 14165), *A. duranensis* (V 14167), and *A. ipaënsis* (K 30076), described previously (Nascimento et al. 2018, 2020) were included in Figure 5 to enable comparison.

Genome-wide SNP analysis of genome stability of induced allotetraploids

It is known that for allotetraploid plants, genetic exchange occurs mainly between chromosomes that are part of the same subgenome, i.e., homologous exchanges. However, it was previously noted that a proportion of these genetic exchanges in allotetraploid *Arachis* happen between different subgenomes (homeologous exchanges) (Leal-Bertioli et al. 2015; Clevenger et al. 2017; Bertioli et al. 2019).

Here, we investigated genome-wide variation in progeny from the two polyploidy events, IpaDur1 and IpaDur2, in different generations: 15 different lines of the first generation (S₁) of IpaDur2 (BBAA genome) and 23 individuals of eight generations of the previously obtained induced allotetraploid IpaDur1 (BBAA genome), using the 48K Affymetrix chip (Korani et al. 2019). Four thousand two hundred and sixty-three polymorphic loci were detected between *A. duranensis* (AA genome) and *A. ipaënsis* (BB genome) and used for genome-wide analysis. Because the current analysis was investigating the autotetraploid-like behavior (recombination between homeologs), the loci were ordered according to the ten

chromosomal pseudomolecules (chr) of *A. ipaënsis*. There was significant variation between IpaDur1 and IpaDur2 individuals (Figure 6). The large majority of loci presented the expected AABB composition, AA from *A. duranensis* and BB from *A. ipaënsis*. However, all chromosomes presented some loci with the composition AAAA or BBBB, indicating homeologous recombination. Two patterns of homeologous recombinations were observed: loci that were interspersed throughout the chromosomes and, the most prevalent, loci that occur in continuous segments, or blocks (e.g., IpaDur2-S₂-pl11 chr A04/B04, Supplementary File S2). The interspersed homeologous loci can be plausibly explained by gene conversion whilst blocks can be plausibly explained by tetrasomic meiotic recombination. The overall rate of homeologous recombination detected for IpaDur2 S₂ was 3.32%, and for all generations of IpaDur1 was 7.76% (Figure 6A). However, this is likely to be underestimated because with SNP chip genotyping is not possible to detect genome changes that result from balanced homeologous exchanges. Homeologous exchange in blocks were mostly detected at the distal parts of the pseudomolecules while interspersed loci were detectable throughout the body of chromosomes (Supplementary File S2).

The chromosomes A04/B04 (42.74%), A06/B06 (16.02%), and A05/B05 (12.14%), which all show a high level of collinearity (Bertioli et al. 2019), had the highest frequency of homeologous recombination for all induced allotetraploids: changes in these chromosomes occurred in all 38 lineages that were randomly chosen for analysis (Figure 6, A and B, Supplementary File S2). Using GISH cytogenetic analysis, chromosomes cyt-B10 of IpaDur1 and IpaDur2 showed mosaic hybridization patterning, suggesting that this is the chromosome with the highest level of genomic exchange between subgenomes, and prevalent invasion

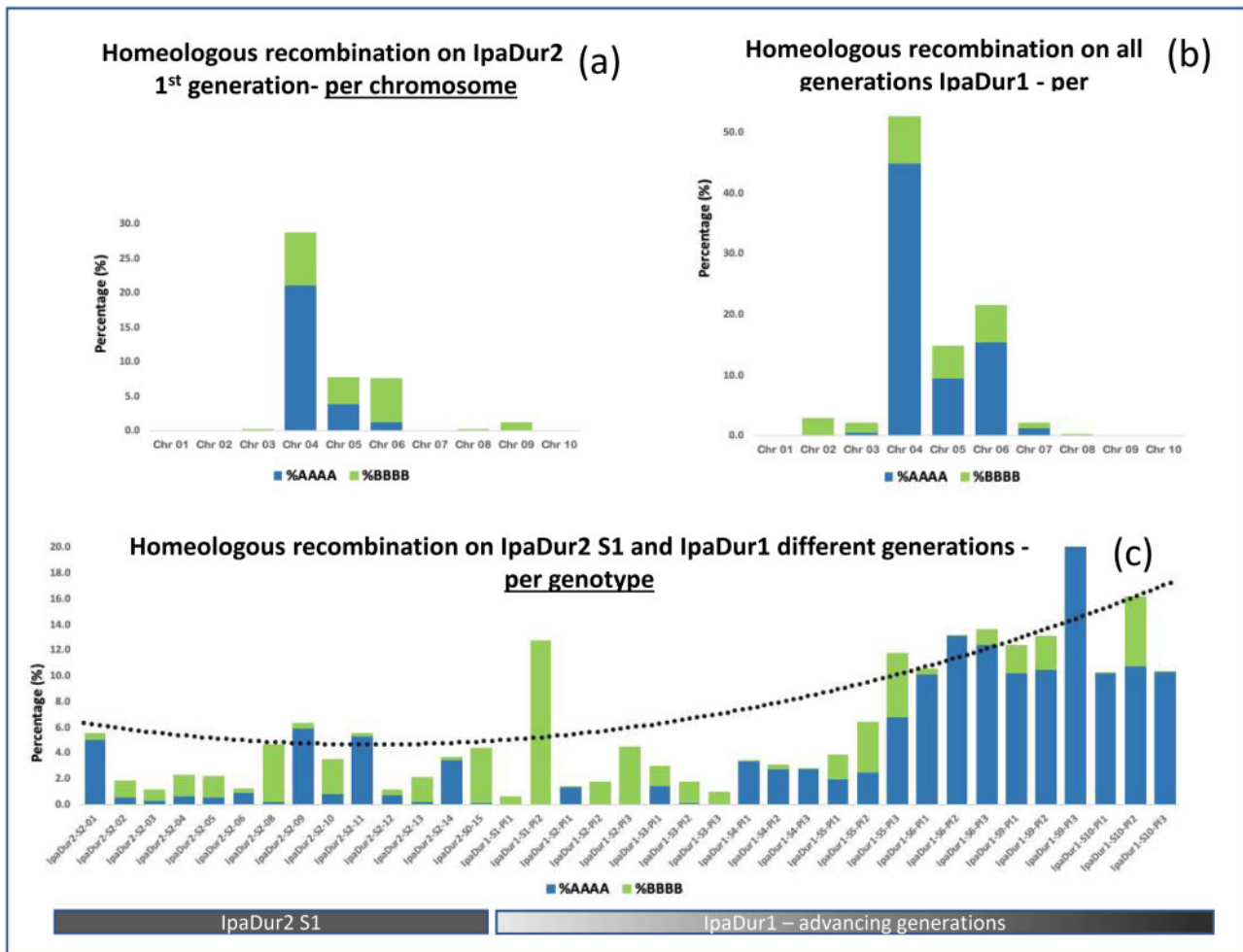


Figure 6 Histograms showing the total percentage of homeologous recombinations: (A) in each chromosome of IpaDur2 first generation; (B) in each chromosome of IpaDur1, an average of six different generations; and (C) on all individuals of all generations. Blue are the conversions from AABB to AAAA, and green, conversions to BBBB. Note that conversion to AAAA is prevalent, Chromosome 4 has most homeologous recombinations and that there is a tendency for individuals of later generations to accumulate more homeologous recombinations.

of A alleles onto the B subgenome (Figure 3). Because genetic and cytogenetic analyses agree, we can plausibly suggest that cyt-B10 corresponds to chromosomal pseudomolecule B04.

There was an overall similar tendency for conversion to AAAA (1.79%) and to BBBB (1.53%) across all chromosomes in IpaDur2 individuals. On IpaDur1, however, there was a much higher rate of conversion to AAAA (5.69%) than to BBBB (2.05%). In all 38 individuals, from both allotetraploids and different generations, exchanges were generally asymmetrical—most genotypes had severe bias to either AAAA or BBBB. The exceptions were IpaDur2 S₂-12 (58.6% AAAA/41.4% BBBB) and IpaDur1 S₇-3 (57.9% AAAA/42.1% BBBB). There was a strong bias towards AAAA (4.77% compared to 2.03% BBBB). Previously it has been shown that *A. hypogaea* has overall bias towards BBBB, but that this tendency was reversed to AAAA towards the chromosome ends (Bertioli et al. 2019).

For IpaDur2 S₂, homeologous recombination ranged from 1.23% to 6.36% throughout the whole genome (average 3.32%). For IpaDur1, where we were able to access different generations, a much wider range was observed: 0.7 (IpaDur1 S₃-1) to 20.08% (IpaDur1S₁₁-3). Homeologous recombination tended to increase over generations (Figure 6C).

Discussion

Peanut is an allotetraploid of recent origin with an AABB type genome ($2n = 4x = 40$). It arose from one, or a very few, events of hybridization between the diploid species *A. duranensis* and *A. ipaënsis* followed by spontaneous tetraploidization (Kochert et al. 1996; Seijo et al. 2007; Bertioli et al. 2016, 2019). Here, we studied induced neotetraploids obtained from the sequenced accessions of the progenitor species (V 14167 and K 30076) in two distinct events (Favero et al. 2006; Bertioli et al. 2019). This gave us the opportunity to observe independently generated lineages and different generations of the same lineage. The first generation of both lineages (IpaDur1 and IpaDur2) showed low germination rate, and highly variable fertility, with some individuals producing no pods at all. However, fertility in later generations recovered. This is consistent with the suggestion made by Ramsey and Schemske (2002) that newly formed allopolyploids have reduced fertility because of unbalanced gametes, but that, genetics permitting, lineages which form balanced gametes are selected. A sufficient level of fertility clearly being a condition for young polyploids to form viable sexually reproducing lineages in the long term. In this study, we show that the induced allotetraploid lineages that

advanced in generations exhibited enhanced diversity in seed size and pod characteristics, flower color, and genome configurations (Figures 1 and 6, Supplementary Materials 2). A similar rapid diversification following the spontaneous formation of the polyploid species, *A. monticola* and *A. hypogaea*, provides a highly plausible mechanism which allowed an allotetraploid, with such narrow genetic origin, to diversify phenotypically and be favored in domestication over much more genetically diverse diploid species.

For several years, it was naïvely assumed that these newly induced allotetraploids had (1) a genome that was the sum of the A and B subgenomes in equal parts, forming an AABB composition in all loci, and (2) followed diploid genetics: that is, homologous chromosomes would exclusively pair at meiosis. However, as the tools for genetic mapping advanced, and denser datasets became available, we discovered that both assumptions were inaccurate. Genome regions with deviant compositions, AAAA or BBBB were detected, demonstrating that homoeologous recombination was surprisingly common (Leal-Bertioli et al. 2015, 2018; Clevenger et al. 2017). Although trivalent and tetravalent chromosome associations had been previously observed during meiosis of cultivated peanut in cytogenetic studies (Husted 1936; Smartt et al. 1978; Singh and Moss 1982; Wynne et al. 1989), the occurrence of homoeologous recombination in genetic studies had gone almost unnoticed before (Leal-Bertioli et al. 2015). The role of homoeologous recombination in the evolution and domestication of several allopolyploids has been well documented, in oilseed rape (*Brassica napus*; Sharpe et al. 1995; Chalhoub et al. 2014; Hurgobin et al. 2018), and in other species, including quinoa (*Chenopodium quinoa*; Jarvis et al. 2017), and tobacco (*Nicotiana tabacum*; Chen et al. 2018). Homoeologous recombination is now thought to not only alter gene dosage of large chromosomal segments but also to provide a mechanism for evolutionary novelty in transcript and protein sequences in nascent allopolyploids, including the formation of intergenomic “recombinant” proteins (Zhang et al. 2020). In this study, we observed the presence of homoeologous recombination in several chromosomes and its consequences at the cytogenetic level.

In 2008, under the scope of the Generation Challenge Programme (www.generationcp.org), seeds of IpaDur1 were distributed to different research groups around the world (in Senegal, France, USA, Argentina), becoming a public resource. With this, independent studies were performed by different groups, with occasional discrepancy in some results. An example is the contrasting results of Nascimento et al. (2018) and Seijo et al. (2018) who did cytogenetic analyses on what was assumed to be the same genotype, IpaDur1. Both groups observed large macrostructural stability of karyotype, however differences were observed in the number of detectable 45S loci. In the work here, we found this very same divergence between different events of tetraploidization of the newly formed IpaDur2, and even between different cells of roots from the same plant: some metaphases showed five, some showed only three 45S rDNA loci (Figure 4). This recurring inconsistency in the number of 45S rDNA sites detected indicates high genome instability in these distinct lineages distributed to both groups. One possibility is that 45S rDNA tandem repeats were lost or reduced in size in cyt-B3 and cyt-B7 in both IpaDur1 and IpaDur2; another is the remodeling of chromatin (Liu and Wendel 2003; Neves et al. 2005; Chiavegatto et al. 2019) that altered probe hybridization or fluorescence detection (also see Gao et al. 2021). These chromosomal changes are consistent with those observed in other recently formed allotetraploids (Xiong et al. 2011; Chester et al. 2015) but contrasts very strongly

to the higher cytogenetic stability generally observed in polyploid crops, including the natural allotetraploids, *A. hypogaea* and *A. monticola* (Nascimento et al. 2018; Bertioli et al. 2019). This corroborates the inference that in early generations high instability naturally occurs, but in later generations, genome becomes stabilized by suppression of homeologous exchange and/or selection of lines with lower levels of chromosome rearrangements (Cifuentes et al. 2010; Zhang et al. 2020). This initial instability would provide phenotypic variation upon with artificial selection could act, thus offering the opportunity for niche expansion in the new allotetraploid species. In a recent review, Van de Peer et al. (2021) also highlighted that the response to biotic and abiotic stresses are important in determining the establishment and success of new polyploids. Such stresses are likely to be encountered in the new ecological niches of domestication and the preferential selection of tetraploid *Arachis* over diploid could result from their more varied and/or improved responses (phenotypic plasticity) awarded by polyploidy.

In addition to cytogenetic characterization, we addressed genome changes by assaying the dosage of single nucleotide polymorphisms (SNPs) which differentiated the two diploid progenitor species in the DNA of 39 lineages derived from two events of polyploidization. In the early generations derived from IpaDur2, we found that between 1.23 and 6.36% of the genome had been impacted by homeologous recombination. That is, the genome had converted from an AABB configuration to AAAA or BBBB. Although variable between lineages, the results with IpaDur1 indicate that this percentage increased in later generations, a characteristic of the polyploid ratchet (Figure 6; Gaeta and Pires 2010). The phenotypic variability observed were differences in germination rate and fertility in early generations, and flower color and seed size in later generations. These can be very plausibly explained by genomic instability. Homoeologous recombination was more frequent in some chromosomes than others. From the sixth generation onwards, for the lineages studied, the chromosome A04/B04 SNP alleles assayed entirely converted to AAAA, a type of “total collapse” (Figure 6A, Supplementary File S2). Notably, however, the chromosomal composition of these lines as observed at the cytogenetic level remained 10 A chromosome pairs, and 10 B chromosome pairs, but with one pair of chromosomes (cyt-B10) showing an interspersed mosaic patterning in GISH. This genomic “collapse” could also account for the viability loss observed in some lineages at S₉ and S₁₀ generations. If, as seems likely, similar genetic instability was present at the origin of *A. hypogaea* and *A. monticola*—how did they regain stability?

Genome instability has, in the past, led some authors to consider polyploidy an “evolutionary dead end” (e.g., Mayrose et al. 2011). However, it is well established that polyploids can survive and flourish with controlling mechanisms to ensure some level of genome stability during regular meiotic division, and consequent fertility. Regular segregation of chromosomes during meiosis requires a restriction of pairing between homoeologous chromosomes to avoid configurations that lead to the production of unbalanced and aneuploid gametes, aneuploid progenies, chromosome rearrangements and reduced fertility (Benavente et al. 2001; Sánchez-Morán et al. 2001; Ramsey and Schemske 2002). To date, only two mechanisms of genome stabilization in allopolyploids have been clearly defined: *differential affinity* and *pairing regulators*. *Differential affinity* [concept by Darlington (1928)] is when differences between the complementary homeologous chromosomes (structural changes and DNA sequence divergence) preclude homoeologous chromosome pairing. In fact, a

study of four wheat allotetraploids showed that instability caused by homoeologous exchange were nonrandomly distributed along the chromosomes. Density of homoeologous exchanges increased on both arms along the centromere–telomere axis, corresponding to genomic regions with higher gene density, higher DNA similarity, lower DNA methylation level, and higher chromatin accessibility (Zhang et al. 2020). Pairing regulators is when genetic systems regulate homoeologous pairing. Such regulators have been identified in several allopolyploid species, such as wheat, where the gene *Ph1* has been shown to contribute to genetic stabilization of wheat by suppressing homoeologous pairing at Meiosis I. In its absence, hexaploid wheat is not able to form stable bivalents (Riley and Chapman 1958; Riley 1960; Griffiths et al. 2006). In addition, over eight genes have been implicated with genome stabilization in the autotetraploid *Arabidopsis arenosa* (Morgan et al. 2020). The relative importance of the genes contributing to the cytological diploidization of polyploids is presumably generally greater with more closely related homoeologous genomes. However, it is not trivial to

disentangle the relative effects of differential affinities and pairing regulator genes (Jenczewski and Alix 2004, Mason and Wendel 2020). In cultivated peanut, there is evidence for both. First, differential affinity may have been enhanced by chromosomal deletions and rearrangements following polyploidy. In particular, it is notable that the inversion in chromosome A05 relative to the sequenced diploid ancestor is immediately adjacent to the largest tetrasomic genome conformation in the tetraploid genome (Bertioli et al. 2019). It is very plausible that this inversion, by disrupting collinearity, could have hindered extensive homoeologous exchange, stabilizing chromosomes A05/B05 from total collapse. Second, the existence of pairing regulators in *Arachis* is implied by the QTLs associated with homoeologous recombination frequency identified in Leal-Bertioli et al. (2015).

It has long been accepted that initial genome duplication event at the origin of peanut created a bottleneck between the domesticated and its diploid wild relatives (Figure 7). We had previously suggested that genetic deletions and exchange between A and B subgenomes generated variation that helped to favor the

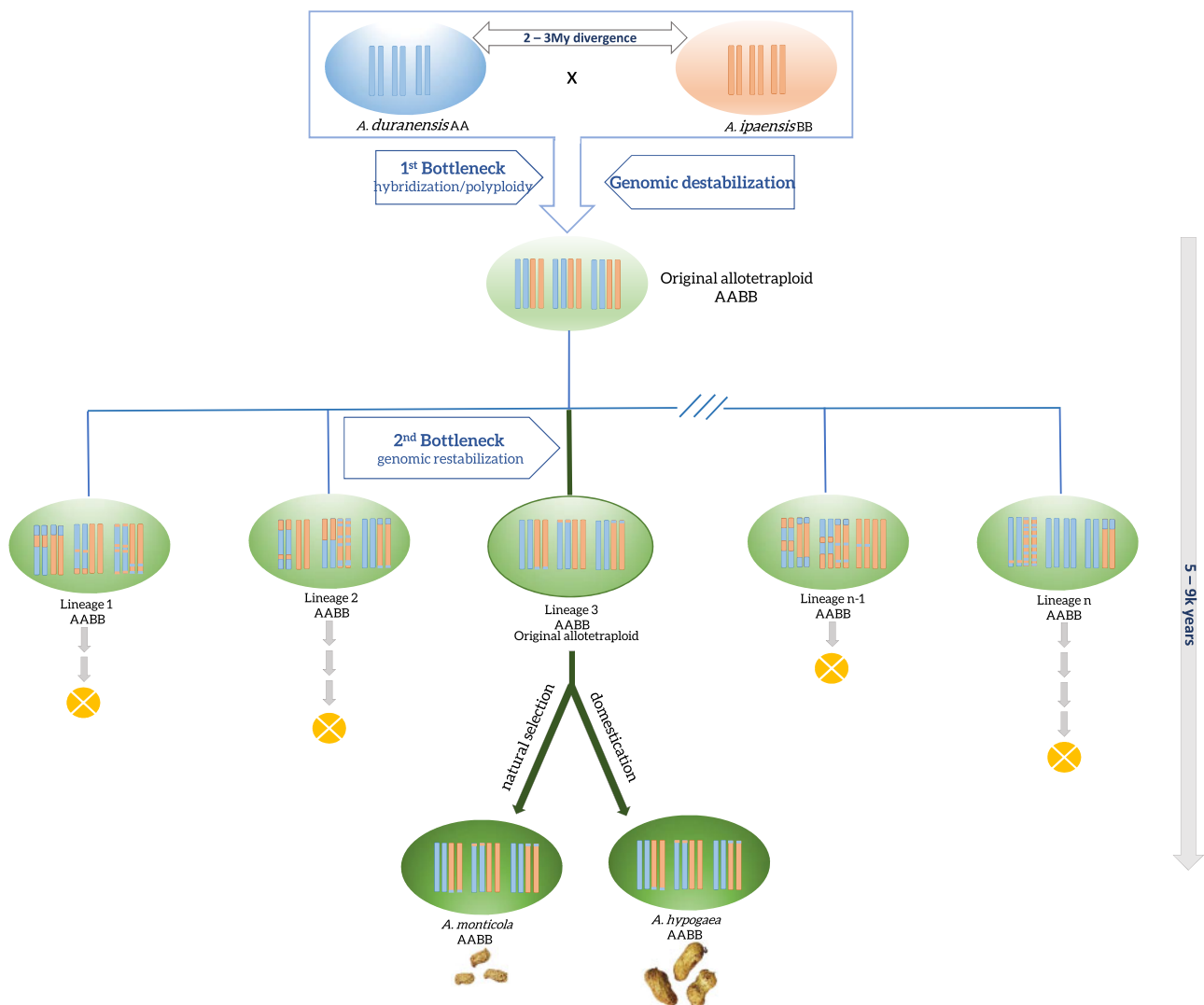


Figure 7 Schematic representation of the origin and evolution of the two spontaneously formed allotetraploids, the wild *A. monticola* and the cultivated peanut, *A. hypogaea*. The diploid *A. duranensis* crosses with *A. ipaensis* to generate a sterile diploid hybrid, that undergoes natural polyploidization. The rarity of this event and the barrier that the ploidy causes characterize the first bottleneck. Lineages originated from the nascent allotetraploid have significant genomic instability (here observed by genotyping and cytogenetics), abnormal chromosome pairing, causing low fertility. Most lineages collapse, except the ones that have efficient mechanisms in place that homoeologous exchange. This survival of only a few lineages represents the second bottleneck in evolution of peanut.

domestication of *A. hypogaea* over its diploid relatives (Bertioli et al. 2019). Here, we further conclude a scenario for the origin of *A. hypogaea* and *A. monticola*: after the initial polyploidization, the resulting individuals underwent a period of genomic instability, generating high phenotypic variability, ranging from individuals with inability to produce seed to those with stabilizing genetic variants. We propose that lineages fit for domestication captured phenotypic variations favorable to cultivation but also stronger genetic mechanisms for limiting genome instability which favored their long-term survival.

Data availability

All data are in the Supplementary Files. Diploid progenitor accessions are available at the USDA-PGRUCU (Plant Genetic Resources Conservation Unit at the United States Department of Agriculture) under accession numbers PI 468322 and PI 692197. Allotetraploids may be obtained from the authors under request. Supplementary material is available at figshare: <https://doi.org/10.25387/g3.14696724>.

Acknowledgments

The authors would like to thank Jenny Leverett and Leandro Mesquita for their technical assistance.

S.L.B., D.J.B., and A.C.G.A. conceived and designed the study; E.B.N. and A.C.G.A. conducted cytogenetic analysis; S.L.B. and D.J.B. performed SNP array analysis, M.C.F.C. did statistical analysis, M.C.M., A.R.C., and M.S.H. conducted phenotyping. S.L.B., D.J.B., E.B.N., and A.C.G.A. drafted the manuscript. All authors were involved in manuscript revision and approved the submitted version.

Funding

This work was supported by Agriculture and Food Research Initiative Competitive Grant no. 2018-67013-28139 co-funded by the USDA National Institute of Food and Agriculture and the National Peanut Board, grants from, Mars Wrigley Inc., Peanut Research Foundation, Coordenação de Aperfeiçoamento de Pessoal de Nível Superior (CAPES) and Fundação de Amparo à Pesquisa do Distrito Federal (FAP-DF).

Conflicts of interest

The authors declare that there is no conflict of interest.

Literature cited

Adams KL, Wendel JF. 2005. Polyploidy and genome evolution in plants. *Curr Opin Plant Biol.* 8:135–141.

Benavente E, Alix K, Dusautoir JC, Orellana J, David JL. 2001. Early evolution of the chromosomal structure of *Triticum turgidum*–*Aegilops ovata* amphiploids carrying and lacking the *Ph1* gene. *Theor Appl Genet.* 103:1123–1128.

Bertioli DJ, Abernathy B, Seijo G, Clevenger J, Cannon SB. 2020. Evaluating two different models of peanut's origin. *Nat Genet.* 52:557–559.

Bertioli DJ, Cannon SB, Froenicke L, Huang G, Farmer AD, et al. 2016. The genome sequences of *Arachis duranensis* and *Arachis ipaensis*, the diploid ancestors of cultivated peanut. *Nat Genet.* 48:438–446.

Bertioli DJ, Jenkins J, Clevenger J, Dudchenko O, Gao D, et al. 2019. The genome sequence of segmental allotetraploid peanut *Arachis hypogaea*. *Nat Genet.* 51:877–884.

Blaine Marchant D, Soltis DE, Soltis PS. 2016. Patterns of abiotic niche shifts in allopolyploids relative to their progenitors. *New Phytol.* 212:708–718.

Chalhoub B, Denoeud F, Liu S, Parkin IAP, Tang H, et al. 2014. Early allopolyploid evolution in the post-Neolithic *Brassica napus* oilseed genome. *Science.* 345:950–953.

Chen S, Ren F, Zhang L, Liu Y, Chen X, et al. 2018. Unstable allotetraploid tobacco genome due to frequent homeologous recombination, segmental deletion, and chromosome loss. *Mol Plant.* 11:914–927.

Chester M, Riley RK, Soltis PS, Soltis DE. 2015. Patterns of chromosomal variation in natural populations of the neoallotetraploid *Tragopogon mirus* (Asteraceae). *Heredity (Edinb).* 114:309–317.

Chiavegatto RB, Chaves ALA, Rocha LC, Benites FRG, Peruzzi L, et al. 2019. Heterochromatin bands and rDNA sites evolution in polyploidization events in *Cynodon Rich.* (Poaceae). *Plant Mol Biol Rep.* 37:477–487.

Cifuentes M, Grandont L, Moore G, Chèvre AM, Jenczewski E. 2010. Genetic regulation of meiosis in polyploid species: new insights into an old question. *New Phytol.* 186:29–36.

Clevenger J, Chu Y, Chavarro C, Agarwal G, Bertioli DJ, et al. 2017. Genome-wide SNP genotyping resolves signatures of selection and tetrasomic recombination in peanut. *Mol Plant.* 10:309–322.

Comai L. 2005. The advantages and disadvantages of being polyploid. *Nat Rev Genet.* 6:836–846.

Darlington CD. 1928. Studies in *Prunus*, I and II. *J Gen.* 19:213–256.

Doyle J, Doyle J. 1987. A rapid DNA isolation procedure for small quantities of fresh leaf tissue. *Phytochem Bull.* 19:11–15.

Favero AP, Simpson CE, Valls JFM, Vello NA. 2006. Study of the evolution of cultivated peanut through crossability studies among *Arachis ipaensis*, *A. duranensis*, and *A. hypogaea*. *Crop Sci.* 46:1546–1552.

Gaeta RT, Pires JC. 2010. Homoeologous recombination in allopolyploids: the polyploid ratchet. *New Phytologist.* 186:18–28.

Gao D, Araujo ACG, Nascimento EFMB, Chavarro MC, Xia H, et al. 2021. ValSten: a new wild species derived allotetraploid for increasing genetic diversity of the peanut crop (*Arachis hypogaea* L.). *Genet Resour Crop Evol.* 68:1471–1485.

García AV, Ortiz AM, Silvestri MC, Custodio AR, Moretzsohn MC, et al. 2020. Occurrence of 2n microspore production in diploid interspecific hybrids between the wild parental species of peanut (*Arachis hypogaea* L., Leguminosae) and its relevance in the genetic origin of the cultigen. *Crop Sci.* 60:2420–2436.

Grabiele M, Chalup L, Robledo G, Seijo G. 2012. Genetic and geographic origin of domesticated peanut as evidenced by 5S rDNA and chloroplast DNA sequences. *Plant Syst Evol.* 2012:1151–1165.

Griffiths S, Sharp R, Foote TN, Bertin I, Wanous M, et al. 2006. Molecular characterization of *Ph1* as a major chromosome pairing locus in polyploid wheat. *Nature.* 439:749–752.

Hurgobin B, Golicz AA, Bayer PE, Chan CK, Timaz S, et al. 2018. Homoeologous exchange is a major cause of gene presence/absence variation in the amphidiploid *Brassica napus*. *Plant Biotechnol J.* 16:1265–1274.

Husted L. 1936. Cytological Studies on The Peanut. *Arachis*. II — Chromosome number, morphology and behavior, and their application to the problem of the origin of the cultivated forms. *Cytologia.* 7:396–423.

Jarvis DE, Ho YS, Lightfoot DJ, Schmöckel SM, Li B, et al. 2017. The genome of *Chenopodium quinoa*. *Nature.* 542:307–312.

- Jenczewski E, Alix K. 2004. From diploids to allopolyploids: the emergence of efficient pairing control genes in plants. *Crit Rev Plant Sci.* 23:21–45.
- Kochert G, Stalker HT, Gimenes M, Galgano L, Lopes CR, et al. 1996. RFLP and cytogenetic evidence on the origin and evolution of allotetraploid domesticated peanut, *Arachis hypogaea* (Leguminosae). *Am J Bot.* 83:1282–1291.
- Korani W, Clevenger JP, Chu Y, Ozias-Akins P. 2019. Machine learning as an effective method for identifying true single nucleotide polymorphisms in polyploid plants. *Plant Genome.* 12:180023.
- Krapovickas A, Gregory WC. 2007. Taxonomy of the genus *Arachis* (Leguminosae). *Bonplandia.* 16:1–205.
- Lashermes P, Combes MC, Hueber Y, Severac D, Dereeper A. 2014. Genome rearrangements derived from homoeologous recombination following allopolyploidy speciation in coffee. *Plant J.* 78:674–685.
- Lavia G, Fernandez A, Seijo J. 2008. Cytogenetic and molecular evidences on the evolutionary relationships among *Arachis* species. *Plant Genome.* 1E:101–134.
- Lavia GI, Ortiz AM, Robledo G, Fernandez A, Seijo G. 2011. Origin of triploid *Arachis pintoi* (Leguminosae) by autopolyploidy evidenced by FISH and meiotic behaviour. *Ann Bot.* 108:103–111.
- Leal-Bertioli S, Shirasawa K, Abernathy B, Moretzsohn M, Chavarro C, et al. 2015. Tetrasomic recombination is surprisingly frequent in allotetraploid *Arachis*. *Genet.* 199:1093–1105.
- Leal-Bertioli SCM, Godoy IJ, Santos JF, Doyle JJ, Guimarães PM, et al. 2018. Segmental allopolyploidy in action: increasing diversity through polyploid hybridization and homoeologous recombination. *Am J Bot.* 105:1053–1066.
- Leal-Bertioli SCM, Moretzsohn MC, Santos SP, Brasileiro AC, Guimarães PM, et al. 2017. Phenotypic effects of allotetraploidization of wild *Arachis* and their implications for peanut domestication. *Am J Bot.* 104:379–388.
- Leitch IJ, Hanson L, Lim KY, Kovarik A, Chase MW, et al. 2008. The ups and downs of genome size evolution in polyploid species of *Nicotiana* (Solanaceae). *Ann Bot.* 101:805–814.
- Levene H. 1960. Robust tests for equality of variances. In: I Olkin, editor. *Contributions to Probability and Statistics: Essays in Honor of Harold Hotelling*. Palo Alto, CA: Stanford University Press. p. 278–292.
- Liu B, Wendel JF. 2003. Epigenetic phenomena and the evolution of plant allopolyploids. *Mol Phylogenet Evol.* 29:365–379.
- Mason AS, Wendel JF. 2020. Homoeologous exchanges, segmental allopolyploidy, and polyploid genome evolution. *Front Genet.* 11:1014.
- Mayrose I, Zhan SH, Rothfels CJ, Magnuson-Ford K, Barker MS, et al. 2011. Recently formed polyploid plants diversify at lower rates. *Science.* 333:1257.
- McClintock B. 1984. The significance of responses of the genome to challenge. *Science.* 226:792–801.
- Moretzsohn MC, Gouvea EG, Inglis PW, Leal-Bertioli SCM, Valls JFM, et al. 2013. A study of the relationships of cultivated peanut (*Arachis hypogaea*) and its most closely related wild species using intron sequences and microsatellite markers. *Ann Bot.* 111:113–126.
- Morgan C, Zhang H, Henry CE, Franklin FCH, Bomblies K. 2020. Derived alleles of two axis proteins affect meiotic traits in autotetraploid *Arabidopsis arenosa*. *Proc Natl Acad Sci USA.* 117:8980–8988.
- Nascimento EFMB, dos Santos BV, Marques LOC, Guimarães PM, Brasileiro ACM, et al. 2018. The genome structure of *Arachis hypogaea* (Linnaeus, 1753) and an induced *Arachis* allotetraploid revealed by molecular cytogenetics. *Comp Cytogenet.* 12:111–140.
- Nascimento EFMB, Leal-Bertioli SCM, Bertioli DJ, Chavarro C, Freitas FO, et al. 2020. Brazilian Kayabi Indian accessions of peanut, *Arachis hypogaea* (Fabales, Fabaceae): origin, diversity and evolution. *Genet Mol Biol.* 43:e20190418.
- Neves N, Delgado M, Silva M, Caperta A, Morais-Cecilio L, et al. 2005. Ribosomal DNA heterochromatin in plants. *Cytogenet Genome Res.* 109:104–111.
- Pedrosa A, Sandal N, Stougaard J, Schweizer D, Bachmair A. 2002. Chromosomal map of the model legume *Lotus japonicus*. *Genetics.* 161:1661–1672.
- Ramos ML, Fleming G, Chu Y, Akiyama Y, Gallo M, et al. 2006. Chromosomal and phylogenetic context for conglutin genes in *Arachis* based on genomic sequence. *Mol Genet Genomics.* 275:578–592.
- Ramsey J, Schemske DW. 1998. Pathways, mechanisms, and rates of polyploid formation in flowering plants. *Annu Rev Ecol Syst.* 29:467–501.
- Ramsey J, Schemske DW. 2002. Neopolyploidy in flowering plants. *Annu Rev Ecol Syst.* 33:589–639.
- Riley R. 1960. The diploidisation of polyploid wheat. *Heredity.* 15:407–429.
- Riley R, Chapman V. 1958. Genetic control of the cytologically diploid behaviour of hexaploid wheat. *Nature.* 182:713–715.
- Robledo G, Lavia G, Seijo G. 2009. Species relations among wild *Arachis* species with the A genome as revealed by FISH mapping of rDNA loci and heterochromatin detection. *Theor Appl Genet.* 118:1295–1307.
- Robledo G, Seijo G. 2008. Characterization of the *Arachis* (Leguminosae) D genome using fluorescence in situ hybridization (FISH) chromosome markers and total genome DNA hybridization. *Genet Mol Biol.* 31:717–724.
- Robledo G, Seijo G. 2010. Species relationships among the wild B genome of *Arachis* species (section *Arachis*) based on FISH mapping of rDNA loci and heterochromatin detection: a new proposal for genome arrangement. *Theor Appl Genet.* 121:1033–1046.
- Sánchez-Morán E, Benavente E, Orellana J. 2001. Analysis of karyotypic stability of homoeologous-pairing (ph) mutants in allopolyploid wheats. *Chromosoma.* 110:371–377.
- Santana SH, Valls JFM. 2015. *Arachis veigae* (Fabaceae), the most dispersed wild species of the genus, and yet taxonomically overlooked. *Bonplandia.* 24:139–150.
- Schwarzacher T, Heslop-Harrison JS. 2000. *Practical In Situ Hybridization*. Oxford, UK: BIOS Scientific Publishers.
- Schweizer D, Ambros PF. 1994. Chromosome banding. Stain combinations for specific regions. *Methods Mol Biol.* 29:97–112.
- Seijo JG, Atahuachi M, Simpson CE, Krapovickas A. 2021. *Arachis inflata*: a new B genome species of *Arachis* (Fabaceae). *Bonplandia.* 30:1–6.
- Seijo JG, Kovalsky EI, Chalup LMI, Samoluk SS, Fávero A, et al. 2018. Karyotype stability and genome-specific nucleolar dominance in peanut, its wild 4× ancestor, and a synthetic AABB polyploid. *Crop Sci.* 58:1671–1683.
- Seijo JG, Lavia GI, Fernandez A, Krapovickas A, Ducasse D, et al. 2004. Physical mapping of the 5S and 18S-25S rRNA genes by FISH as evidence that *Arachis duranensis* and *A. ipaënsis* are the wild diploid progenitors of *A. hypogaea* (Leguminosae). *Am J Bot.* 91:1294–1303.
- Seijo JG, Lavia GI, Fernandez A, Krapovickas A, Ducasse DA, et al. 2007. Genomic relationships between the cultivated peanut (*Arachis hypogaea*, Leguminosae) and its close relatives revealed by double GISH. *Am J Bot.* 94:1963–1971.

- Sharpe AG, Parkin IA, Keith DJ, Lydiate DJ. 1995. Frequent nonreciprocal translocations in the amphidiploid genome of oilseed rape (*Brassica napus*). *Genome*. 38:1112–1121.
- Silvestri MC, Ortiz AM, Lavia GI. 2015. rDNA loci and heterochromatin positions support a distinct genome type for 'x = 9 species' of section *Arachis* (*Arachis*, Leguminosae). *Plant Syst Evol*. 301:555–562.
- Singh AK, Moss JP. 1982. Utilization of wild relatives in genetic improvement of *Arachis hypogaea* L. *Theor Appl Genet*. 61:305–314.
- Smartt J, Gregory WC. 1967. Interspecific cross-compatibility between the cultivated peanut (*A. hypogaea*) and other members of the genus *Arachis*. *Oleagineux*. 22:455–459.
- Smartt J, Gregory WC, Gregory MP. 1978. The genomes of *Arachis hypogaea*. 1. Cytogenetic studies of putative genome donors. *Euphytica*. 27:665–675.
- Soltis PS, Marchant DB, Van de Peer Y, Soltis DE. 2015. Polyploidy and genome evolution in plants. *Curr Opin Genet Dev*. 35:119–125.
- Soltis PS, Soltis DE. 2016. Ancient WGD events as drivers of key innovations in angiosperms. *Curr Opin Plant Biol*. 30:159–165.
- Stalker HT. 1991. A new species in section *Arachis* of peanuts with a D genome. *Am J Bot*. 78:630–637.
- Stebbins GL. 1971. *Chromosomal Evolution in Higher Plants*. London: Edward Arnold.
- Valls JFM, Costa LC, Custodio AR. 2013. A novel trifoliolate species of *Arachis* (Fabaceae) and further comments on the taxonomic section *Trierectoides*. *Bonplandia*. 22:91–97.
- Valls JFM, Simpson CE. 2005. New species of *Arachis* L. (Leguminosae) from Brazil, Paraguay and Bolivia. *Bonplandia*. 14:35–63.
- Valls JFM, Simpson CE. 2017. A new species of *Arachis* (fabaceae) from Mato Grosso, Brazil, related to *Arachis matiensis*. *Bonplandia*. 26:143–150.
- Van de Peer Y, Ashman T-L, Soltis PS, Soltis DE. 2021. Polyploidy: an evolutionary and ecological force in stressful times. *Plant Cell*. 33:11–26.
- Van de Peer Y, Mizrahi E, Marchal K. 2017. The evolutionary significance of polyploidy. *Nat Rev Genet*. 18:411–424.
- Wanzenböck E-M, Schöfer C, Schweizer D, Bachmair A. 1997. Ribosomal transcription units integrated via T-DNA transformation associate with the nucleolus and do not require upstream repeat sequences for activity in *Arabidopsis thaliana*. *Plant J*. 11:1007–1016.
- Wendel JF. 2015. The wondrous cycles of polyploidy in plants. *Am J Bot*. 102:1753–1756.
- Wendel JF, Doyle JJ. 2005. Polyploidy and evolution in plants. In: RJ Henry, editor. *Plant Diversity and Evolution – Genotypic and Phenotypic Variation in Higher Plants*. Wallingford, UK: Cabi Publishing. p. 97–117.
- Wynne JC, Haiward T, Knauff DA. 1989. Genetics and cytogenetics of *Arachis*. *Crit Rev Plant Sci*. 8:189–220.
- Xiong Z, Gaeta RT, Pires JC. 2011. Homoeologous shuffling and chromosome compensation maintain genome balance in resynthesized allopolyploid *Brassica napus*. *Proc Natl Acad Sci USA*. 108:7908–7913.
- Yin D, Ji C, Song Q, Zhang W, Zhang X. 2020. Comparison of *Arachis monticola* with diploid and cultivated tetraploid genomes reveals asymmetric subgenome evolution and improvement of peanut. *Adv Sci*. 7:1901672.
- Yoo MJ, Szadkowski E, Wendel JF. 2013. Homoeolog expression bias and expression level dominance in allopolyploid cotton. *Heredity* (Edinb). 110:171–180.
- Zhang Z, Gou X, Xun H, Bian Y, Ma X, et al. 2020. Homoeologous exchanges occur through intragenic recombination generating novel transcripts and proteins in wheat and other polyploids. *Proc Natl Acad Sci USA*. 117:14561–14571.

Communicating editor: J. Wendel